# Stress-Induced MazF-Mediated Proteins in *Escherichia coli*

Akanksha Nigam,[a] Tamar Ziv,[b] Adi Oron-Gottesman,[a] Hanna Engelberg-Kulka[a]

[a]Department of Microbiology and Molecular Genetics, IMRIC, The Hebrew University Hadassah Medical School, Jerusalem, Israel
[b]Smoler Proteomics Center, Faculty of Biology, Technion, Haifa, Israel

**ABSTRACT** *Escherichia coli mazEF* is an extensively studied stress-induced toxin-antitoxin (TA) system. The toxin MazF is an endoribonuclease that cleaves RNAs at ACA sites. By that means, under stress, the induced MazF generates a stress-induced translation machinery (STM) composed of MazF-processed mRNAs and selective ribosomes that specifically translate the processed mRNAs. Here, we performed a proteomic analysis of all the *E. coli* stress-induced proteins that are mediated through the chromosomally borne *mazF* gene. We show that the mRNAs of almost all of them are characterized by the presence of an ACA site up to 100 nucleotides upstream of the AUG initiator. Therefore, under stressful conditions, induced MazF processes mRNAs that are translated by STM. Furthermore, the presence of the ACA sites far upstream (up to 100 nucleotides) of the AUG initiator may still permit translation by the canonical translation machinery. Thus, such dual-translation mechanisms enable the bacterium under stress also to prepare proteins for immediate functions while coming back to normal growth conditions.

**IMPORTANCE** The stress response, the strategy that bacteria have developed in order to cope up with all kinds of adverse conditions, is so far understood at the level of transcription. Our previous findings of a uniquely modified stress-induced translation machinery (STM) generated in *E. coli* under stress by the endoribonucleolytic activity of the toxin MazF opens a new chapter in understanding microbial physiology under stress at the translational level. Here, we performed a proteomic analysis of all the *E. coli* stress-induced proteins that are mediated by chromosomally borne MazF through STM.

**KEYWORDS** bacterial stress response, toxin-antitoxin, proteomics

Toxin-antitoxin (TA) systems are abundant on the chromosomes of most bacteria. Among these, the first one discovered and the one most studied is *Escherichia coli mazEF* (1). *mazF* specifies for the stable toxin MazF, and *mazE* specifies for the labile antitoxin MazE that interferes with MazF toxicity. MazE is degraded by protease ClpPA (1). *E. coli mazEF* is triggered by various stressful conditions, including DNA damage caused by treatment with nalidixic acid (NA) (2, 3).

*E. coli* MazF was first described as a sequence-specific mRNA endoribonuclease (designated mRNA interferase) that preferentially cleaves mRNAs at ACA sites, thereby inhibiting protein synthesis (4). Subsequently, we found that *E. coli* MazF also targets the 16S rRNA within the 30S ribosomal subunit at the decoding center, thereby removing 43 nucleotides from the 3′ terminus (5). The region removed includes the anti-Shine-Dalgarno (anti-SD) region, resulting in the production of deficient ribosomes. Thus, under stressful conditions, when MazF is induced, special translation machinery, the STM system, is generated. It is composed of (i) MazF, which generates mRNAs by cleaving at ACA sites immediately adjacent to or upstream from the AUG start codons of specific mRNAs (5, 6), and (ii) deficient ribosomes that are selectively able to translate the processed mRNAs (5, 7). Thus, under stress, the

induction of MazF leads to the generation of a novel MazF regulon that is translated by the novel stress ribosomes, resulting in the production of stress proteins.

Pulsed stable-isotope labeling in tissue culture (SILAC) was used in several studies for identifications of newly synthesized proteins (8–11) but rarely in bacterial systems (12). Here, we used this technique to perform a proteomic analysis of the stress-induced proteins whose translation was mediated by chromosomally borne *mazF* in *E. coli*.

## RESULTS

**Characterization of *E. coli* proteins induced by a DNA-damaging agent and mediated by chromosomally borne *mazEF*.** In our experiments, we used *E. coli* strain MC4100 *relA*+ and compared it to its Δ*mazEF* deletion derivative. To damage the DNA, we used nalidixic acid (NA), which, in previous work we found to be an efficient inducer of *mazF* (2). To conduct our proteomic analysis, we used the pulsed SILAC approach. In those experiments, heavy (H) lysine and arginine (containing heavy isotopes of carbon and nitrogen) were added to the medium for a short time. Proteins synthesized after exposure to heavy amino acids contained heavy lysine and arginine, whereas proteins synthesized prior to that time contained only light (L) variants. We determined the relative amounts of newly synthetized proteins in the mutant and wild-type (WT) samples following NA treatment by comparing a naturally occurring light isotope and a heavy new protein (H/L ratio). Previous studies done in vertebrate cells were analyzed after several hours. In our bacterial system, we checked several time points and deduced that 5 min is the optimal time point to figure out which are the differential new proteins. Several (1,949) proteins were identified, and in 832 of them, newly synthetized heavy proteins were detected in one of the samples. We repeated the experiments 3 times and looked for proteins that were induced more in the WT than in the Δ*mazEF* mutants in all the repeats (see Fig. S1 in the supplemental material). Table 1 represents the list of proteins that were induced by the NA treatment in the WT. The list of proteins induced by NA treatment was obtained by comparing the H/L values from all the WT samples to those of the mutant samples. We obtained a total of 42 proteins, many of which are known to participate in the stress response (Fig. 1; see also Discussion). Remarkably, with the exception of six of them, in all the corresponding mRNAs specifying these proteins, the MazF cleavage site ACA was found to be located up to 100 nucleotides upstream of the AUG initiator. It seems that the presence of these ACAs upstream of the AUG initiator is important for the expression of the described stress-induced MazF-mediated proteins. We also carried bioinformatics studies of all *E. coli* genes that carry an ACA site to 100 nucleotides upstream of the AUG initiator. We found that 2,807 genes encode a free region upstream. Among them, 2,229 have an ACA site to 100 nucleotides. Since in our proteomic study only 42 proteins were detected (Table 1), we assume that the existence of an ACA site upstream of the initiation codon is necessary but not enough for the synthesis of the stress-induced MazF-mediated proteins *in E. coli*. Alternatively, the proteins may simply not have been expressed or were degraded under the conditions being studied.

**The distance of an ACA site upstream of the AUG initiator is important for the expression of a stress-induced MazF-mediated protein.** To test whether the expression of a stress-induced MazF-mediated protein is a function of the number of nucleotides between the AUG initiator and the ACA MazF cleavage site, we used a green fluorescent protein (GFP) reporter system (Fig. 2A). In previous work (13), we constructed a similar GFP reporter system in which we demonstrated that *mazF*-mediated expression depends on the existence of an ACA MazF cleavage site upstream from the AUG initiator codon, permitting the generation of a MazF-processed mRNA that is translated by the STM. Here, we studied whether the distance of the ACA site from the AUG initiator plays such a crucial role in the expression of the stress-induced GFP reporter. The results are shown in Fig. 2B, where NA-induced samples are shown in green and the uninduced are shown in blue. As a control, we used this GFP reporter but without any ACA sites upstream from the AUG initiator (Fig. 2B, blue bars). As expected, under stressful conditions, which were obtained by the application of NA, a decrease in

**TABLE 1** Proteins induced in *E. coli* by chromosomally borne *mazF* after nalidixic acid treatment[a]

| Gene name | Protein product | Relative intensity of new protein increment or comment | Possible cutting site | Distance of the possible cutting sites from the AUG initiator (nt) |
|---|---|---|---|---|
| *bolA* | DNA-binding transcriptional regulator | 2.22 | ACA | 29 |
| *cfa* | Cyclopropane-fatty-acyl-phospholipid synthase | 1.4 | ACU | 2 |
| *clpB* | Chaperone protein ClpB | 3.3 | ACA | 86 |
| *clpX* | ATP-dependent Clp protease ATP-binding subunit ClpX | 1.69 | ACA | 20 |
| *def* | Peptide deformylase | 1.28 | ACA | 15 |
| *dksA* | RNA polymerase binding transcription factor | 1.95 | ACA | 1 |
| *dnaK* | Chaperone protein | 3.66 | ACA | 33 |
| *dps* | DNA protection during starvation protein | 2.32 | ACA | 20 |
| *ftsH* | ATP-dependent zinc metalloprotease FtsH | 9.96 | ACA | 1 |
| *galF* | UTP-glucose-1-phosphate uridylyltransferase | 1.52 | ACA | 15 |
| *galU* | UTP-glucose-1-phosphate uridylyltransferase | 1.46 | ACA | 18 |
| *gpml* | 2,3-Bisphosphoglycerate-independent phosphoglycerate mutase | 1.29 | ACU | 15 |
| *groL* | 60-kDa chaperonin | 3.46 | ACA | 25 |
| *groS* | 10-kDa chaperonin | 2.46 | ACA | 32 |
| *grpE* | Protein GrpE | 2.09 | ACA | 90 |
| *hslU* | ATP-dependent protease ATPase subunit | 2.41 | ACA | 19 |
| *ibpA* | Small heat shock protein | 1.86 | ACA | 30 |
| *ihfB* | Integration host factor | 1.60 | ACA | 40 |
| *infC* | Translation initiation factor IF-3 | 1.36 | ACA | 18 |
| *lon* | Lon protease | 5.8 | ACA | 50 |
| *metK* | *S*-Adenosylmethionine synthase | 1.64 | ACA | 40 |
| *osmC* | Peroxiredoxin | 1.7 | ACA | 2 |
| *osmE* | Osmotically inducible lipoprotein E | 4.58 | ACA | 14 |
| *osmY* | Osmotically inducible protein Y | 2.78 | ACA | 13 |
| *pckA* | Phosphoenolpyruvate carboxykinase | 3.79 | ACA | 23 |
| *pflB* | Formate acetyltransferase 1 | 1.76 | ACA | 1 |
| *rho* | Transcription termination factor | 1.40 | ACA | 7 |
| *rplU* | 50 S ribosomal protein | 1.57 | ACU | 42 |
| *rpmA* | 50 S ribosomal protein | 1.43 | ACA | 89 |
| *rpoD* | RNA polymerase sigma factor | 1.92 | ACA | 35 |
| *rraB* | Regulator of ribonuclease activity | 1.79 | ACA | 18 |
| *sra* | Stationary-phase-induced ribosome-associated protein | 1.55 | ACA | 18 |
| *tas* | Protein Tas | 1.44 | ACG | 5 |
| *tyrB* | Aromatic-amino-acid aminotransferase | 8.6 | ACA | 74 |
| *upp* | Uracil phosphoribosyl transferase | Expressed only in MC4100 *relA*+ | ACG | 81 |
| *ybeD* | Uncharacterized protein | 3.84 | ACA | 1 |
| *ybeZ* | PhoH-like protein | 1.94 | ACA | 17 |
| *ycaC* | Uncharacterized protein | Expressed only in MC4100 *relA*+ | ACA | 93 |
| *ydfG* | NADP-dependent 3-hydroxy acid dehydrogenase | 1.83 | ACA | 7 |
| *yeeX* | Uncharacterized protein | 1.43 | ACA | 19 |
| *ygaU* | Uncharacterized protein | 2.27 | ACA | 37 |
| *yqjD* | Uncharacterized protein | 1.66 | ACU | 2 |

[a]*E. coli* strain MC4100 *relA*+ and its Δ*mazEF* derivative were grown to mid-logarithmic phase (OD$_{600}$, 0.5). Both cultures were treated with 100 $\mu$g/ml of nalidixic acid (NA) for 10 min at 37°C without shaking. The heavy amino acids arginine ($_{15}$N$^4$) and lysine ($_{15}$N$^2$) were added to both the NA-induced cultures at a concentration of 100 $\mu$g/ml and further incubated at 37°C for 5 min. Cells were centrifuged and sent for proteomic analysis. The table demonstrates the relative intensities of new protein increment in the H/L ratio of MC4100 *relA*+ divided by the H/L ratio of its Δ*mazEF* derivative. The data represent the means of results from triplicate experiments. The last column shows the numbers of nucleotides (distance) from the possible cutting sites to the AUG initiator of each mRNA. nt, nucleotides.

GFP expression was observed (Fig. 2B, the green bars on the left), probably due to the inability of the reporter to be efficiently translated by the STM system. In contrast, the presence of an ACA site up to 80 nucleotides upstream of the AUG initiator permitted an increase in GFP expression following induction with NA (Fig. 2B, compare green bars to blue bars). In contrast, when we inserted an ACA site at 20, 40, or 80 nucleotides upstream from the AUG initiator, induction by NA led to an increase in GFP expression (green bars). On the other hand, a decrease in GFP expression was found when the ACA sites were located at a distance of ≥100 nucleotides upstream of the AUG initiator (Fig. 2B), indicating that the existence of an ACA site within 80 to 100 nucleotide upstream of the AUG initiator is important for the generation of a MazF-processed
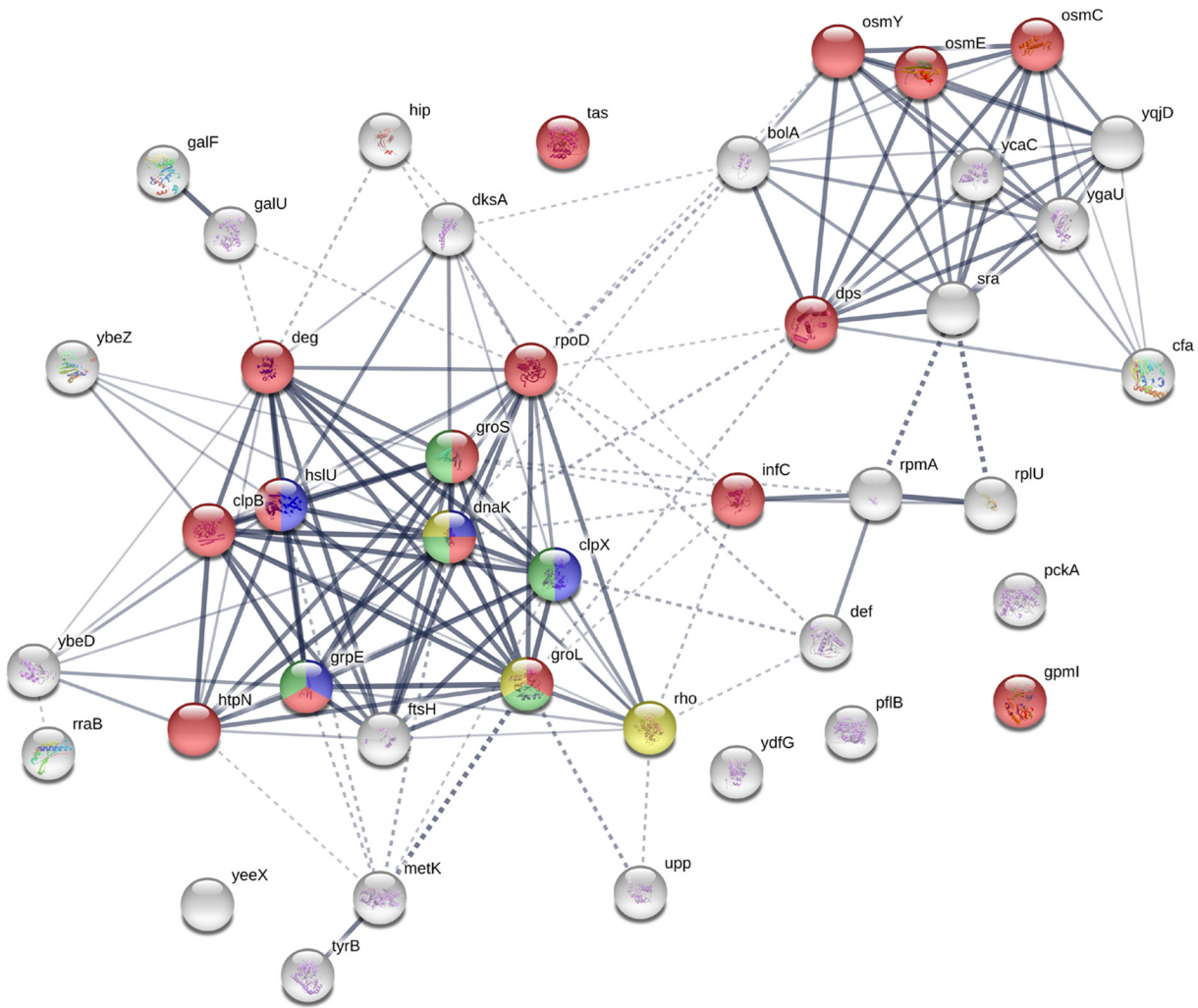
**FIG 1** Interaction map and annotation enrichment of the newly synthesized *mazEF*-related proteins. String software was used to analyze the interactions. The nodes are colors based on the enriched annotations as detailed here. For Gene Ontology Biological Process (GOBP) identifier (ID) 0043335, the pathway was protein unfolding, the gene count was 4, the FDR was 3.19e−05, and the color is blue. For GOBP ID 0006950, the pathway was response to stress, the gene count was 16, the FDR was 0.00567, and the color is red. For GOBP ID 0019538, the pathway was protein metabolic process, the gene count was 14, the FDR was 0.015, and the color is green. For GOBP ID 0006457, the pathway was protein folding, the gene count was 5, the FDR was 0.0324, and the color is light green. For KEGG ID 03018, the pathway was RNA degradation, the gene count was 3, the FDR was 0.0445, and the color is yellow. For InterPro ID IPR003959, the pathway was ATPase with the AAA-type core, the gene count was 5, the FDR was 9.23e−06, and the color is pink.

mRNA and thereby for being preferentially translated by the STM system. These results corroborate our findings that most (85%) of the stress-induced MazF-mediated proteins described here (Table 1) were specified by mRNAs in which there were ACA sites within 93 nucleotides upstream from the AUG initiator.

## DISCUSSION

Here, we report our proteomic analysis of the entire group of *E. coli* proteins that are stress induced and MazF mediated (Table 1). That the proteins described really are MazF mediated is supported by two lines of evidence. (i) We compared results for *E. coli* strain MC4100 *relA*+ and for its deletion derivative MC4100 *relA*+ Δ*mazEF*, and proteomics was carried out on proteins whose increment of expression by the stress-induced conditions (application of NA) was above 1.2. Levels of expression vary between 1.28 and 9.96 and were an average of results from three independent experiments. (ii) About 85% of these proteins (Table 1) were found to be programmed by mRNAs carrying the ACA MazF cleavage site located at least 100 nucleotides upstream from the AUG
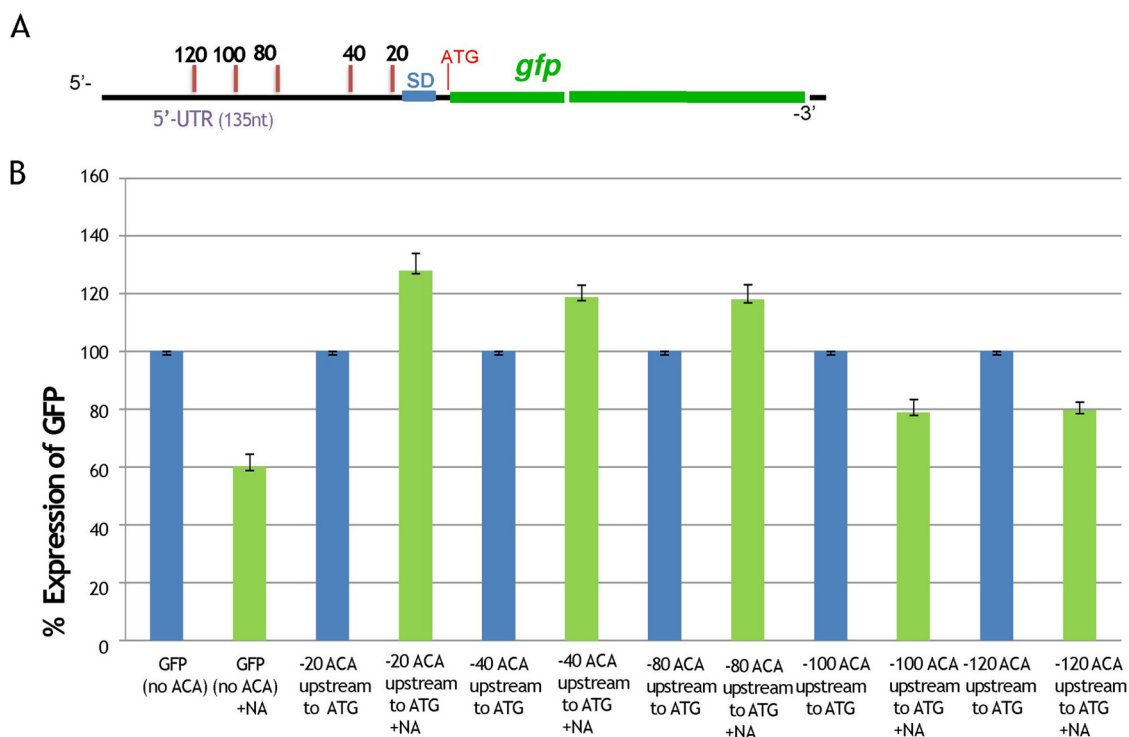
**FIG 2** The distance of the ACA site from the AUG initiation codon plays a role in the expression of the stress-induced GFP reporter. (A) GFP reporter system for studying the effect of the location of ACA sites upstream from the AUG initiation codon on translation under stress. We used a *gfp* reporter gene that carries no ACA sites in its coding sequence and no ACA sites upstream (up to 135 nucleotides) from the ATG initiation codon (13). We used this reporter system as a basis for generating five new constructs. In each new construct, we inserted an ACA site upstream from the ATG initiation codon at specific locations, nucleotides 20, 40, 80, 100, and 120. 5′-UTR, 5′ untranslated region. (B) Levels of GFP expression as a result of the location of the ACA site upstream from the AUG initiation codon. *E. coli* strain MG1655 was separately transformed with plasmid pUH-C carrying five different *gfp* reporter genes with an ACA site upstream from the initiation codon, ATG. Here we show a quantitative comparison of levels of GFP expression in samples induced by nalidixic acid (green bars) and in uninduced samples (blue bars). These data were calculated as percentages of fluorescence units. For each assay, 100% represents the results for the untreated sample.

initiation codon. These results corroborated with previous findings showing that in *E. coli*, under stressful conditions, MazF induction leads to the generation of the new translation machinery, STM, translating mRNAs carrying the MazF cleavage site ACA up to 100 nucleotides upstream of their AUG initiation codons (6). Still, here we found that about 15% of the stress-induced MazF-mediated proteins were translated from mRNAs without an ACA codon within 100 nucleotides upstream from the AUG initiation codon (Table 1); instead, they were translated from mRNAs carrying either an ACG or an ACU site. ACG and ACU are cleavage sites for the toxin ChpBK of the *chpBIK* TA system (14). Just as stressful conditions induce MazF activity, it is possible that similar stressful conditions induce *chpBIK* to generate ChpBK. ChpBK cleaving the mRNA molecule at the upstream ACG or ACU site would result in translation by the STM. Alternatively, the already stress-induced MazF might induce ChpBK synthesis, leading to cleavage upstream at ACG or ACU, again leading to translation by the STM.

In conclusion, most of the MazF-induced proteins characterized here contain an ACA motif within 100 nucleotides upstream of the AUG initiator (except for the few that use ACG or ACU). Thus, as previously reported (5–7), the upstream ACA motif is important for the translation by the stress-induced MazF-mediated machinery (STM). However, our data do not rule out the possibility of additional recognition motifs, and we are currently pursuing these.

In addition, many of the proteins characterized here have previously been described as stress-induced proteins. These include a group of chaperon-related proteins that participate in the prevention of protein unfolding occurring under stress. This category includes proteins ClpB (15), DnaK (16), GroL and GroS (17), and GrpE (18). The stress-induced proteins

also include three proteases: (i) Lon, which is required for cellular homeostasis and for survival from DNA damage and developmental changes induced by stress (19); (ii) ClpX, which specifies components of the Clp protease complex (20); and (iii) FtsH, an ATP-dependent metalloprotease (21). The stress-induced proteins also include one heat shock protein, IbpA (22), proteins involved in carbohydrate metabolism, like GalU (23) and phosphoenolpyruvate carboxylase PckA (24), and three osmotic proteins, OsmC (25), OsmE (26), and OsmY (27). Another key protein is the DNA-binding protein from starved cells (Dps), which was shown to be involved in protection from multiple stresses (28).

However, it may be that the most interesting proteins that were obtained in our studies are those that are self-evidently also produced under regular (unstressed) growth conditions. In this category we can include (i) the well-known RNA polymerase sigma factor RpoD, which promotes the attachment of RNA polymerase to initiation sites (29, 30); (ii) translation initiation factor IF-3 (directed by *infC*), one of the essential components for the initiation of protein synthesis (31); (iii) transcription termination factor Rho (32); (iv) the 50S ribosomal proteins RplU and RpmA (33); and (v) 30S ribosomal protein Sra (34). These proteins, which are so central to bacterial survival, are synthesized under normal unstressed conditions by the canonical translation system. Under stressful conditions, however, when their mRNAs are processed by MazF at an ACA codon located upstream from its initiator, translation can take place by the STM system. Thus, we suggest that the location of the ACA site upstream of the AUG initiator may allow the protein to be synthesized both under stress conditions by STM and under normal conditions by the canonical translation machinery. Such dual-translation mechanisms enable the cells to prepare proteins for immediate functions while coming back from stressful conditions to normal growth conditions.

## MATERIALS AND METHODS

**Bacterial strains and plasmids.** We used *E. coli* MC4100 *relA*+ and its Δ*mazEF* derivative MC4100 *relA*+ Δ*mazEF* (35), *E. coli* MG1655 (13), and plasmid pUH-C (13).

**Characterizing the *E. coli* proteins induced by MazF under stressful conditions.** Early-logarithmic cells of either *E. coli* MC4100 *relA*+ or MC4100 *relA*+ Δ*mazEF* were grown in M9 minimal medium (without lysine and arginine) at 37°C until an optical density at 600 nm ($OD_{600}$) of 0.5 was reached. Stressful conditions were generated by adding 100 $\mu$g/ml of nalidixic acid (NA) for 10 min, after which heavy arginine ($_{15}N^4$) and heavy lysine ($_{15}N^2$) were added at a concentration of 100 $\mu$g/ml to each of the cultures, which were further incubated without shaking for 5 min. Samples of these treated cultures were centrifuged, frozen in liquid nitrogen, and sent to the Smoler Protein Research Center in Haifa, Israel, for proteomic analysis.

**Experimental design and statistical rationale.** This study consists of proteome analyses of two group types, *E. coli* MC4100 *relA*+ and MC4100 *relA*+Δ*mazEF*, to discover newly synthetized proteins by pulsed SILAC. Triplicate samples from each group were examined, with each replicate pair being examined on different dates. Liquid chromatography-tandem mass spectrometry (LC-MS/MS) data from all 3 experiments were combined and analyzed. Peptide and protein–level false discovery rates (FDRs) were filtered to 1% by using the target decoy strategy for identification. H/L ratios for all peptides belonging to a particular protein species were pooled; a ratio for each protein in each sample was calculated separately. As the purpose of the study was to identify the new proteins rather than to calculate the turnover of the proteins, no complex statistical test was used and no logarithmic transformation was done.

More-detailed information is provided in the following sections.

**Proteolysis and mass spectrometry analysis.** The proteins were extracted from the cell pellets in 9 M urea, 400 mM ammonium bicarbonate, 10 mM dithiothreitol (DTT), with 2 cycles of sonication. Ten micrograms of protein from each sample was reduced (60°C for 30 min), modified with 35 mM iodoacetamide in 400 mM ammonium bicarbonate (in the dark at room temperature for 30 min), and digested in 2 M urea, 80 mM ammonium bicarbonate with modified trypsin (Promega) at a 1:50 enzyme-to-substrate ratio overnight at 37°C. An additional second trypsinization was done for 4 h after diluting the urea concentration to 1 M.

The resulting tryptic peptides were desalted using $C_{18}$ tips (Harvard) dried and resuspended in 0.1% formic acid. They were analyzed by LC–MS/MS using a Q Exactive Plus mass spectrometer (Thermo) fitted with a capillary high-performance liquid chromatograph (HPLC; easy nLC 1000; Thermo). The peptides were loaded onto a homemade capillary column (25-cm, 75-$\mu$m internal diameter) packed with Reprosil $C_{18}$–Aqua (Dr. Maisch GmbH, Ammerbuch, Germany) in solvent A (0.1% formic acid in water). The peptide mixture was resolved with a (5 to 28%) linear gradient of solvent B (95% acetonitrile with 0.1% formic acid) for 105 min, followed by a 15-min gradient of 28 to 95% and 15 min at 95% acetonitrile with 0.1% formic acid in water at flow rates of 0.15 $\mu$l/min. Mass spectrometry was performed in a positive mode (*m/z* 350 to 1,800; resolution, 70,000) using a repetitively full MS scan followed by collision–induced dissociation (high-energy collision dissociation [HCD], at a normalized collision energy of 35) of the 10 most dominant ions (> 1 charges) selected from the first MS scan. The AGC settings were 3 × 10⁶ for the

**TABLE 2** Primers used

| Primer | Sequence |
|---|---|
| P**F** ACA 20up | GGCGTATTTTG**ACA**CCTAACGAGG |
| P**R** ACA 20up | CCTCGTTAGG**TGT**CAAAATACGCC |
| P**F** ACA 40up | CTCGTTGGAG**ACA**TTCATGGCGT |
| P**R** ACA 40up | ACGCCATGAA**TGT**CTCCAACGAG |
| P**F** ACA 80up | ATATTGAGCAG**ACA**CCCCGGTGAAG |
| P**R** ACA 80up | CTTCACCGGGG**TGT**CTGCTCAATAT |
| P**F** ACA 100up | CGAAGATATCG**ACA**GAGTTAATAT |
| P**R** ACA 100up | ATATTAACTC**TGT**CGATATCTTCG |
| P**F** ACA 120up | GGGGTGCTCG**ACA**TAAGCCGAAG |
| P**R** ACA 120up | CTTCGGCTTA**TGT**CGAGCACCCC |

full MS scan and $1 \times 10^5$ for the MS/MS scans. The intensity threshold for triggering MS/MS analysis was $1 \times 10^4$. A dynamic exclusion list was enabled with an exclusion duration of 20 s.

The mass spectrometry data of all 3 repeats were analyzed using MaxQuant software v.1.5.2.8. (36) for peak picking identification and quantitation using the Andromeda search engine, which searches for tryptic peptides against the *Escherichia coli* K-12 UniProt database (4,459 entries), with mass tolerances of 20 ppm for the precursor masses and 20 ppm for the fragment ions. Oxidation on methionine and protein N terminus acetylation were accepted as variable modifications, and carbamidomethyl on cysteine was accepted as a static modification, as the percentage of the carbamylation was very low. Minimal peptide length was set to 6 amino acids, and a maximum of two miscleavages was allowed. Peptide– and protein–level false discovery rates (FDRs) were filtered to 1% using the target decoy strategy. Protein tables were filtered to eliminate the identifications from the reverse database and common contaminants and single peptide identifications. The data were quantified by SILAC analysis using the same software. H/L ratios for all peptides belonging to a particular protein species were pooled, providing a ratio for each protein.

**Construction of GFP reporters for studying the effect of ACA sites upstream of the AUG initiator on GFP.** To construct the genes for our green fluorescent protein (GFP) reporters, we previously used a GFP variant derived from Emerald-GFP (EmGFP; pRSET-*em-gfp*; Invitrogen, Carlsbad, CA, USA). Emerald-GFP has a distinct excitation peak at 487 nm and a distinct emission peak at 509 nm. In this *gfp* gene, we changed all the ACA sites to ATA sites, thus eliminating all MazF cleavage sites while maintaining the protein coding sequence (13). Moreover, this GFP reporter gene carries no ACA sites upstream of the initiation codon ATG (up to 135 nucleotides). The *gfp* construct was cloned into a pUH-C plasmid (13). Here, we used this *gfp* construct as a platform to insert ACA sites upstream of the initiation codon ATG at 5 different locations. The ACA codons were inserted at different distances (numbers of nucleotides) upstream of the initiation codon ATG: –20, –40, –80, –100, and –120 nucleotides.

In order to create each ACA insertion, a forward primer (PF) and a reverse primer (PR) were designed. PCRs were carried out using the *gfp* construct carrying no ACA sites (on a pUH-C plasmid) as a template. To create newly mutated synthesized plasmids and to prevent extra mutations, we carried out the PCR program with only a few cycles of annealing: 5 cycles for the first annealing stage and 10 cycles for the second annealing stage. Finally, to eliminate the original plasmid and leave only newly mutated synthesized unmethylated plasmids, we added the enzyme DpnI to cut the methylated DNA, leaving the unmethylated DNA intact. We confirmed all of the generated mutations by sequencing.

We inserted ACA sites at each of five specific locations, 20, 40, 80, 100, and 120 nucleotides upstream from the ATG initiation codon, by using the primers in Table 2.

**Growth conditions and assays for measuring GFP expression.** We used plasmids bearing each of the *gfp* reporter genes to transform *E. coli* MG1655 (WT). We grew the transformed bacteria in 10 ml M9 medium containing 0.2% glucose and 100 $\mu$g/ml ampicillin at 37°C with shaking (250 rpm) until the cultures reached an $OD_{600}$ of 0.4 to 0.5. Using black 96-well plates, we applied triplicate samples to wells, not treating the controls and treating the experimental samples with 100 $\mu$g/ml of NA to induce MazF activity. We detected GFP levels using a FLUOstar spectrophotometer. Using a 485 $\pm$ 15 nm excitation filter and a 520 $\pm$ 15 nm emission filter over a total time of 750 min, we measured fluorescence 150 times at intervals of 300 s (total time of experiment, 750 min). We maintained the temperature in the device at 37°C. The GFP fluorophore was excited with 1,000-CW lamp energy, and the fluorescence in each well was measured for 5 s (FLUOstar galaxy; BMG Labtech).

**Data availability.** The mass spectrometry proteomics data have been deposited in the Proteome-Xchange Consortium (http://proteomecentral.proteomexchange.org) via the PRIDE partner repository with the data set identifier PXD010101.

## SUPPLEMENTAL MATERIAL

Supplemental material for this article may be found at https://doi.org/10.1128/mBio .00340-19.

**FIG S1**, TIF file, 0.01 MB.

**TABLE S1**, XLSX file, 0.8 MB.

**TABLE S2**, XLSX file, 6.6 MB.

## REFERENCES

1. Aizenman E, Engelberg-Kulka H, Glaser G. 1996. An *Escherichia coli* chromosomal "addiction module" regulated by guanosine-3′5′-bispyrophosphate: a model for programmed bacterial cell death. Proc Natl Acad Sci U S A 93:6059–6063. https://doi.org/10.1073/pnas.93.12.6059.

2. Hazan R, Sat B, Engelberg-Kulka H. 2004. *Escherichia coli* mazEF mediated cell death is triggered by various stressful conditions. J Bacteriol 186:3663–3669. https://doi.org/10.1128/JB.186.11.3663-3669.2004.

3. Godoy VG, Jarosz DF, Walker FL, Simmons LA, Walker G. 2006. Y-family DNA polymerases respond to DNA damage-independent inhibition of replication fork progression. EMBO J 25:868–879. https://doi.org/10.1038/sj.emboj.7600986.

4. Zhang Y, Zhang J, Hara H, Kato I, Inouye M. 2005. Insight into mRNA cleavage mechanism by MazF, an mRNA interferase. J Biol Chem 280:3143–3150. https://doi.org/10.1074/jbc.M411811200.

5. Vesper O, Amitai S, Belitsky M, Byrgazov K, Kaberdina AC, Engelberg-Kulka H, Moll I. 2011. Selective translation of leaderless mRNAs by specialized-ribosomes generated by MazF in *Escherichia coli*. Cell 147:147–111. https://doi.org/10.1016/j.cell.2011.07.047.

6. Sauert M, Wolfinger MT, Vesper O, Müller C, Byrgazov K, Moll I. 2016. The MazF-regulon: a toolbox for the post-transcriptional stress response in *Escherichia coli*. Nucleic Acids Res 44:6660–6675. https://doi.org/10.1093/nar/gkw115.

7. Moll I, Engelberg-Kulka H. 2012. Selective translation during stress in *Escherichia coli*. Trends Biochem Sci 296:493–498. https://doi.org/10.1016/j.tibs.2012.07.007.

8. Selbach M, Schwanhäusser B, Thierfelder N, Fang Z, Khanin R, Rajewsky N. 2008. Widespread changes in protein synthesis induced by micro-RNAs. Nature 455:58–63. https://doi.org/10.1038/nature07228.

9. Schwanhäusser B, Busse D, Li N, Dittmar G, Schuchhardt J, Wolf J, Chen W, Selbach M. 2011. Global quantification of mammalian gene expression control. Nature 473:337–342. https://doi.org/10.1038/nature10098.

10. Cambridge SB, Gnad F, Nguyen C, Bermejo JL, Krüger M, Mann M. 2011. Systems-wide proteomic analysis in mammalian cells reveals conserved, functional protein turnover. J Proteome Res 10:5275–5284. https://doi.org/10.1021/pr101183k.

11. Cohen LD, Zuchman R, Sorokina O, Müller A, Dieterich DC, Armstrong JD, Ziv T, Ziv NE. 2013. Metabolic turnover of synaptic proteins: kinetics, interdependencies and implications for synaptic maintenance. PLoS One 8:e63191. https://doi.org/10.1371/journal.pone.0063191.

12. Chua SL, Yam JK, Hao P, Adav SS, Salido MM, Liu Y, Givskov M, Sze SK, Tolker-Nielsen T, Yang L. 2016. Selective labelling and eradication of antibiotic-tolerant bacterial populations in Pseudomonas aeruginosa biofilms. Nat Commun 197:10750. https://doi.org/10.1038/ncomms10750.

13. Oron-Gottesman A, Sauert M, Engelberg-Kulka H, Moll I. 2016. Stress-induced bias in the reading of the genetic code in Escherichia coli. mBio 7:e01855-16. https://doi.org/10.1128/mBio.01855-16.

14. Zhang Y, Zhu L, Zhang J, Inouye M. 2005. Characterization of ChpBK, an mRNA interferase from *Escherichia coli*. J Biol Chem 280:26080–26088. https://doi.org/10.1074/jbc.M502050200.

15. Barnett ME, Zolkiewska A, Zolkiewski M. 2000. Structure and activity of ClpB from *Escherichia coli*. Role of the amino- and carboxyl-terminal domains. J Biol Chem 275:37565–37571. https://doi.org/10.1074/jbc.M005211200.

16. Mashaghi A, Bezrukavnikov S, Minde DP, Wentink AS, Kityk R, Zachmann-Brand B, Mayer MP, Kramer G, Bukau B, Tans SJ. 2016. Alter-native modes of client binding enable functional plasticity of Hsp70. Nature 539:448–451. https://doi.org/10.1038/nature20137.

17. Fenton WA, Horwich AL. 2003. Chaperone-mediated protein folding: fate of substrate polypeptide. Q Rev Biophys 36:229–256. https://doi.org/10.1017/S0033583503003883.

18. Yoshimune K, Yoshimura T, Nakayama T, Nishino T, Esaki N. 2002. Hsc62, Hsc56, and GrpE, the third Hsp70 chaperone system of *Escherichia coli*. Biochem Biophys Res Commun 293:1389–1395. https://doi.org/10.1016/S0006-291X(02)00403-5.

19. Wohlever ML, Baker TA, Sauer RT. 2014. Roles of the N domain of the AAA+ Lon protease in substrate recognition, allosteric regulation and chaperone activity. Mol Microbiol 91:66–78. https://doi.org/10.1111/mmi.12444.

20. Gottesman S, Clark WP, de Crecy-Lagard V, Maurizi MR. 1993. ClpX, an alternative subunit for the ATP-dependent Clp protease of Escherichia coli. Sequence and in vivo activities. J Biol Chem 268:22618–22626.

21. Tomoyasu T, Gamer J, Bukau B, Kanemori M, Mori H, Rutman AJ, Oppenheim AB, Yura T, Yamanaka K, Niki H, Hiraga S, Ogura T. 1995. *Escherichia coli* FtsH is a membrane-bound, ATP-dependent protease which degrades the heat-shock transcription factor sigma 32. EMBO J 14:2551–2560. https://doi.org/10.1002/j.1460-2075.1995.tb07253.x.

22. Kuczyńska-Wiśnik D, Kedzierska S, Matuszewska E, Lund P, Taylor A, Lipińska B, Laskowska E. 2002. The Escherichia coli small heat-shock proteins IbpA and IbpB prevent the aggregation of proteins denatured in vivo during extreme heat shock. Microbiology 148:1757–1765. https://doi.org/10.1099/00221287-148-6-1757.

23. Marolda CL, Valvano MA. 1996. The GalF protein of *Escherichia coli* is not a UDP-glucose pyrophosphorylase but interacts with the GalU protein possibly to regulate cellular levels of UDP-glucose. Mol Microbiol 22:827–840. https://doi.org/10.1046/j.1365-2958.1996.01531.x.

24. Goldie H, Medina V. 1990. Physical and genetic analysis of the phosphoenolpyruvate carboxykinase (*pckA*) locus from *Escherichia coli* K12. Mol Gen Genet 220:191–196.

25. Shin DH, Choi IG, Busso D, Jancarik J, Yokota H, Kim R, Kim SH. 2004. Structure of OsmC from *Escherichia coli*: a salt-shock-induced protein. Acta Crystallogr D Biol Crystallogr 60:903–911. https://doi.org/10.1107/S0907444904005013.

26. Gutierrez C, Gordia S, Bonnassie S. 1995. Characterization of the osmotically inducible gene *osmE* of *Escherichia coli* K-12. Mol Microbiol 16:553–563. https://doi.org/10.1111/j.1365-2958.1995.tb02418.x.

27. Yim HH, Villarejo M. 1992. *osmY*, a new hyperosmotically inducible gene, encodes a periplasmic protein in *Escherichia coli*. J Bacteriol 174:3637–3644. https://doi.org/10.1128/jb.174.11.3637-3644.1992.

28. Karas VO, Westerlaken I, Meyer AS. 2015. The DNA-binding protein from starved cells (Dps) utilizes dual functions to defend cells against multiple stresses. J Bacteriol 197:3206–3215. https://doi.org/10.1128/JB.00475-15.

29. Maciag A, Peano C, Pietrelli A, Egli T, De Bellis G, Landini P. 2011. In vitro transcription profiling of the σS subunit of bacterial RNA polymerase: re-definition of the σS regulon and identification of σS-specific promoter sequence elements. Nucleic Acids Res 39:5338–5355. https://doi.org/10.1093/nar/gkr129.

30. Goldman SR, Nair NU, Wells CD, Nickels BE, Hochschild A. 2015. The primary σ factor in Escherichia coli can access the transcription elongation complex from solution in vivo. Elife 4:e10514. https://doi.org/10.7554/eLife.10514.

31. Liveris D, Schwartz JJ, Geertman R, Schwartz I. 1993. Molecular cloning

and sequencing of infC, the gene encoding translation initiation factor IF3, from four enterobacterial species. FEMS Microbiol Lett 112:211–216. https://doi.org/10.1111/j.1574-6968.1993.tb06450.x.

32. Skordalakes E, Berger JM. 2003. Structure of the Rho transcription terminator: mechanism of mRNA recognition and helicase loading. Cell 114:135–146. https://doi.org/10.1016/S0092-8674(03)00512-9.

33. Walleczek J, Martin T, Redl B, Stoeffler-Meilicke M, Stoeffler G. 1989. Comparative cross-linking study on the 50S ribosomal subunit from *Escherichia coli*. Biochemistry 28:4099–4105. https://doi.org/10.1021/bi00435a071.

34. Izutsu K, Wada C, Komine Y, Sako T, Ueguchi C, Nakura S, Wada A. 2001.

*Escherichia coli* ribosome-associated protein SRA, whose copy number increases during stationary phase. J Bacteriol 183:2765–2773. https://doi.org/10.1128/JB.183.9.2765-2773.2001.

35. Kolodkin-Gal I, Hazan R, Gaathon A, Carmeli S, Engelberg-Kulka H. 2007. A linear penta-peptide is a quorum sensing factor required for mazEF-mediated cell death in Escherichia coli. Science 318:652–655. https://doi.org/10.1126/science.1147248.

36. Cox J, Mann M. 2008. MaxQuant enables high peptide identification rates, individualized p.p.b.-range mass accuracies and proteome-wide protein quantification. Nat Biotechnol 26:1367–1372. https://doi.org/10.1038/nbt.1511.